# Solution NMR Evidence That the HIV-1 Protease Catalytic Aspartyl Groups Have Different Ionization States in the Complex Formed with the Asymmetric Drug KNI-272

**ARTICLE** *in* BIOCHEMISTRY · SEPTEMBER 1996

Impact Factor: 3.02 · DOI: 10.1021/bi961268z · Source: PubMed



**8 AUTHORS**, INCLUDING:

Darón I Freedberg
U.S. Food and Drug Administration
**52** PUBLICATIONS **1,584** CITATIONS
SEE PROFILE

Stephen J Stahl
U.S. Department of Health and Human Services
**121** PUBLICATIONS **7,269** CITATIONS
SEE PROFILE

Biochemistry

 Volume 35, Number 31 August 6, 1996

*Accelerated Publications*

# Solution NMR Evidence That the HIV-1 Protease Catalytic Aspartyl Groups Have Different Ionization States in the Complex Formed with the Asymmetric Drug KNI-272†

Yun-Xing Wang,‡ Darón I. Freedberg,‡ Toshimasa Yamazaki,‡ Paul T. Wingfield,§ Stephen J. Stahl,§ Joshua D. Kaufman,§ Yoshiaki Kiso,|| and Dennis A. Torchia*,‡

*Molecular Structural Biology Unit, NIDR, Protein Expression Laboratory, NIAMS, National Institutes of Health, Bethesda, Maryland 20892, and Department of Medicinal Chemistry, Kyoto Pharmaceutical University, Yamashina-ku, Kyoto 607, Japan*

*Received May 29, 1996; Revised Manuscript Received June 20, 1996*⊗

ABSTRACT: In order to improve the design of HIV-1 protease inhibitors, it is essential to understand how they interact with active site residues, particularly the catalytic Asp25 and Asp125 residues. KNI-272 is a promising, potent HIV-1 protease inhibitor ($K_i \approx 5$ pM), currently undergoing phase 1 clinical trials. Because KNI-272 is asymmetric, the complex it forms with the homodimeric HIV-1 protease also lacks symmetry, and the two protease monomers can have distinct NMR spectra. Monomer specific signal assignments were obtained for amino acid residues in the drug binding site as well as for six of the eight Asp residues in the protease/KNI-272 complex. Using these assignments, the ionization states of the Asp carboxyl groups were determined from measurements of (a) the pD dependence of the chemical shifts of the Asp carboxyl carbons and (b) the H/D isotope effect upon the Asp carboxyl carbon chemical shifts. The results of these measurements indicate that the carboxyl of Asp25 is protonated while that of Asp125 is not protonated. These findings provide not only the first experimental evidence regarding the distinct protonation states of Asp25/125 in HIV-1 protease/drug complexes, but also shed light on interactions responsible for inhibitor binding that should form the basis for improved drug designs.

HIV-1 protease is a primary target for rationally designed drugs directed against the AIDS virus. This is the case because the protease plays an essential role in the viral life cycle, and inhibition of this enzyme results in the production of noninfectious virions (Huff, 1991). In addition, high-resolution crystal structures are available of both the free protease and the protease complexed with a variety of inhibitors (Wlodawer & Erickson, 1993). The availability of this structural information has stimulated structure-based design of highly specific and potent inhibitors of the enzyme. The X-ray data reveal that the free protease homodimer forms a 2-fold symmetric structure with a catalytic site consisting of two hairpins, containing residues Asp25, Thr26, and Gly27 of one monomer and the corresponding residues of the other monomer, designated Asp125, Thr126, and Gly127 (Wlodaw-

† This work was supported by the AIDS Targeted Antiviral Program of the Office of the Director of the National Institutes of Health.

* To whom correspondence should be addressed at Building 30/Room 132, NIDR, National Institutes of Health, Bethesda, MD 20892-4320. Phone : (301) 496-5750. FAX: (301) 402-1512.

‡ Molecular Structural Biology Unit, NIDR, NIH.

§ Protein Expression Laboratory, NIAMS, NIH.

|| Kyoto Pharmaceutical University.

⊗ Abstract published in *Advance ACS Abstracts,* August 1, 1996.

[1] Abbreviations: NMR, nuclear magnetic resonance; NOESY, nuclear overhauser effect spectroscopy; HSQC: heteronuclear single-quantum correlation spectroscopy; HIV-1, human immunodeficiency virus, type 1; ppm, parts per million.

S0006-2960(96)01268-8 CCC: $12.00 

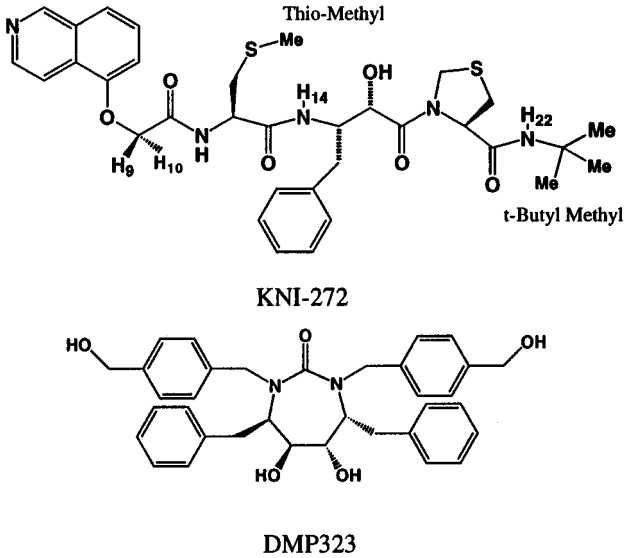


FIGURE 1: Chemical structure of KNI-272. Protons H10, H14, H22 and the protons of the *tert*-Butyl group and the thiomethyl group are labeled, and their NOE cross-peaks to the amide protons of Asp29 and Asp129, Asp30, and Asp130 are shown in Figure 3. For comparison, we also show the chemical structure of DMP323.

er et al., 1989). All potent inhibitors interact with the catalytic carboxyls of Asp25/125. Hence in order to rationally design inhibitors that maximize such interactions, it is necessary to have information about the ionization states and p$K_a$ values of the catalytic Asp carboxyls. Such information is difficult to obtain in direct fashion from X-ray data, because protons are not observed in protein electron density maps. In addition, molecular dynamics calculations have predicted that the catalytic aspartyl ionization states, at a given external pH, will vary according to the specific interactions experienced by the Asp side chains in each protease/inhibitor complex (Harte & Beveridge, 1993).

High-resolution $^1H-^{13}C$ multidimensional NMR is well suited to follow the pH titration of Asp and Glu carboxyl side chains in proteins (Oda et al., 1993). A recent study of the protease complexed with a potent, 2-fold symmetric inhibitor, DMP323 showed that both Asp25 and Asp125 are protonated over the pH range extending from 2.2 to 7.0 (Yamazaki et al., 1994b). DMP323 is a member of the cyclic urea class of inhibitors in which two hydroxyl groups are fixed to the urea ring in positions to interact symmetrically with the two catalytic aspartyl groups (Lam et al., 1994). An asymmetric but nonetheless highly potent protease inhibitor, KNI-272, is a substrate-based, peptidomimetic transition state mimic (Kiso, 1996) whose chemical structure contrasts markedly with that of DMP323 (Figure 1). KNI-272 is highly selective and nontoxic, with favorable therapeutic indices and pharmacokinetic behavior in animals (Kageyama et al., 1993). It is currently undergoing phase 1 clinical trials (Chokeijichai et al., 1995). A 2.0 Å X-ray crystal structure of the protease/KNI-272 complex has been solved (Baldwin et al., 1995), providing a structural basis for understanding the potency of this novel inhibitor. Quantum chemistry calculations applied to heavy atom coordinates of the crystal structure (Baldwin et al., 1995) have predicted that the Asp25 side chain in one monomer is protonated whereas the Asp125 in the other is not. Herein, we report an NMR titration study of the Asp carboxyls of the protease/KNI-272 complex, which provides the first experimental measurements of p$K_a$ values and ionization states of all Asp carboxyls. These experimental results are compared with the predictions of the quantum chemistry calculations and with the previous experimental results obtained for the protease/DMP323 complex, in order to enhance our understanding of the protease active-site/inhibitor interactions.

## MATERIALS AND METHODS

*Sample Preparation.* The HIV-1 protease is that of the HXB2 isolate with Cys to Ala substitutions at positions 67 and 95. The fully $^{13}C$- and $^{15}N$-labeled recombinant HIV-1 protease was prepared as described previously (Yamazaki

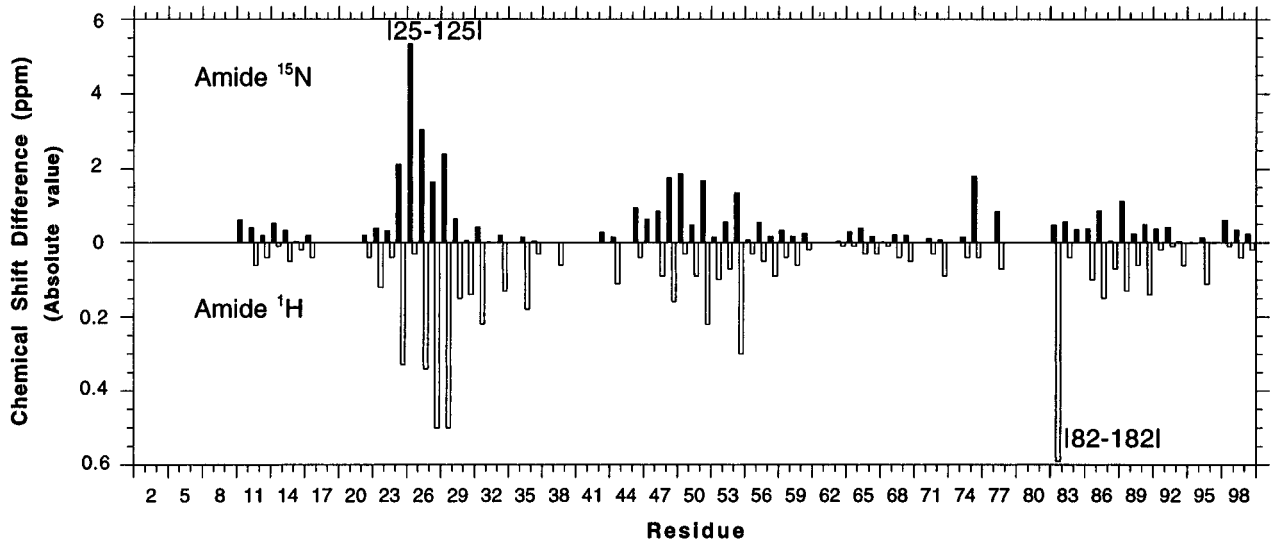


FIGURE 2: Comparison of the amide $^{15}N$ and amide proton chemical shift differences between the two monomers. The differences in chemical shifts are set to zero if assignments are not available, as is the case, for example, for proline residues. Because differences in amide $^1H/^{15}N$ chemical shifts typically reflect differences in local environment, the chemical shift differences are greatest for residues in close contact with KNI-272. For example, the largest differences of the amide $^{15}N$ and $^1H$ chemical shifts are seen for residues Asp25 and Asp125 and Val82 and Val182, respectively. A more detailed interpretation of the chemical shift differences must await the development of a quantitative theory of amide chemical shifts. Note that the bars representing the $^{15}N$ and $^1H$ chemical shift differences are not collinear, and the residue numbers fall between each pair of tick marks.

et al., 1996). NMR spectra were taken on a ~230 $\mu$L solution containing 50 mM NaAc, 0.8 mM protein dimer in a 5 mm Shigemi NMR tube.

*NMR Spectroscopy*. All NMR spectra were recorded on a Bruker AMX500 spectrometer, except for the HCCH-TOCSY spectrum, which was recorded on a Bruker AMX600 spectrometer. Both spectrometers were equipped with carbon optimized, triple-resonance ($^1$H$-^{13}$C$-^{15}$N) probes and pulsed *z*-gradients. For signal assignments, all spectra were taken at 34 °C and were processed on SUN Sparc stations using nmrPipe (Delaglio et al., 1995). Sequential, but not monomer-specific, assignments of ca. 95% of the protease $^1$H, $^{13}$C, and $^{15}$N signals were obtained from multidimensional NMR experiments (Table S1, supporting information) and as described previously (Yamazaki et al., 1994a). Chemical shifts were referenced as in Yamazaki et al. (1994b).

The p$K_a$ values of the aspartic acid carboxyls of the protease/KNI-272 complex were determined by measuring chemical shifts of Asp C$^\gamma$ signals as a function of pD (uncorrected pH meter reading). The uncorrected pH meter readings were used because the isotope effects on a glass electrode and the carboxyl ionization constant nearly cancel (Bundi & Wüthrich, 1979). To maximize sensitivity, 2D HCABGCO spectra (Yamazaki et al., 1994b) were recorded at 45 °C, as the Asp 25/125 C$^\gamma$ signals were extremely weak or unobservable in 3D spectra recorded at 34 °C.

Ionization states and p$K_a$ values of individual Asp residues can be determined only after monomer specific sequential signal assignments are available. Monomer specific assignments present a challenge because the 2-fold chemical shift degeneracy of the HIV protease homodimer NMR signals is only partially lifted when the protease is bound to KNI-272. This is illustrated in Figure 2 where the absolute values of the chemical shift differences of equivalent residues in the two monomers (e.g., Asp25 and Asp125) are plotted as a function of residue number for the amide $^{15}$N and amide $^1$H signals. As expected, large differences in chemical shifts are observed for residues that interact with the inhibitor in the crystal structure, for example, Asp25/125 and Val82/182 (Baldwin et al., 1995). However, other pairs of residues at equivalent positions in the protein sequence that are remote from the inhibitor often have indistinguishable chemical shifts. Hence, while it is straightforward to sequentially assign a string of residues that have non-degenerate chemical shifts, it is significantly more difficult to assign two such strands to a specific monomer when they are separated by a sequence of residues having degenerate chemical shifts in the two monomers. This problem was solved by using the crystal structure of the protease/KNI-272 complex to assign long-range NOEs, observed in a 3D $^{15}$N-edited NOESY-HMQC spectrum. These assignments were used to link the sequentially assigned signals within each monomer. The final step required identification of each monomer with respect to the inhibitor. This was done by first assigning the proton signals of the bound inhibitor using a combination of 2D $^{13}$C-filtered COSY, $^{13}$C-filtered NOESY, 3D $^{13}$C-filtered HMQC-NOESY, and 3D $^{13}$C-filtered and $^{15}$N-edited NOESY spectra.[2] The latter two spectra were then used together with the X-ray coordinates to identify the NOEs between the protons of the unlabeled KNI-272 molecule and the protons in individual monomer strands of the fully labeled protease (Figures 3 and 4). Note that this assignment procedure requires only that there be an approximate correspondence of the solution and crystal structures. For example, in the crystal structure the NH protons of D129 and D130 are ca. 3 Å from the thiomethyl protons of KNI-272 but are over 10 Å from the *tert*-butyl protons. The opposite is true for the amide protons of D29 and D30. Hence the Asp129 and Asp130 amide signals are clearly distinguished from those of Asp29 and Asp30 by the cross-peaks

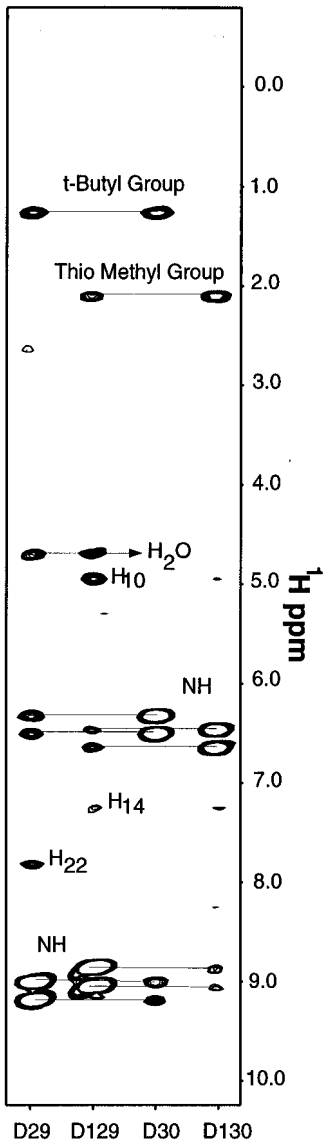


FIGURE 3: Four strips taken from the 3D $^{13}$C-filtered $^{15}$N-edited NOESY spectrum. This spectrum provides NOEs between sequential amide protons as well as NOEs to nonlabeled KNI-272 protons. The strips show, for example, NOEs from the amide proton of Asp29 to the *tert*-Butyl group and to the H23 amide proton of KNI-272 and NOEs from the amide proton of Asp129 to the thiomethyl protons, to a methylene proton, and to the NH14 amide proton of KNI-272.

[2] A 2D $^{13}$C-filtered COSY experiment selectively detects cross-peaks of the unlabeled inhibitor, while filtering out cross-peaks from protons attached to $^{13}$C-labeled protein carbons (Ikura & Bax, 1992); a 2D $^{13}$C-filtered NOESY experiment selectively detects NOE cross-peaks between dipolar coupled protons of an unlabeled inhibitor, while filtering cross-peaks of the isotope-labeled protein protons (Ikura & Bax, 1992); the 3D $^{13}$C-edited HMQC-NOESY experiment selectively detects NOE cross-peaks between protons of the inhibitor and protons attached to $^{13}$C in the labeled protein (Burgering et al., 1993); the 3D $^{15}$N-edited $^{13}$C-filtered NOESY experiment selectively detects NOE cross-peaks between protons of the inhibitor and $^{15}$N-attached amide protons of the protein (Burgering et al., 1993).

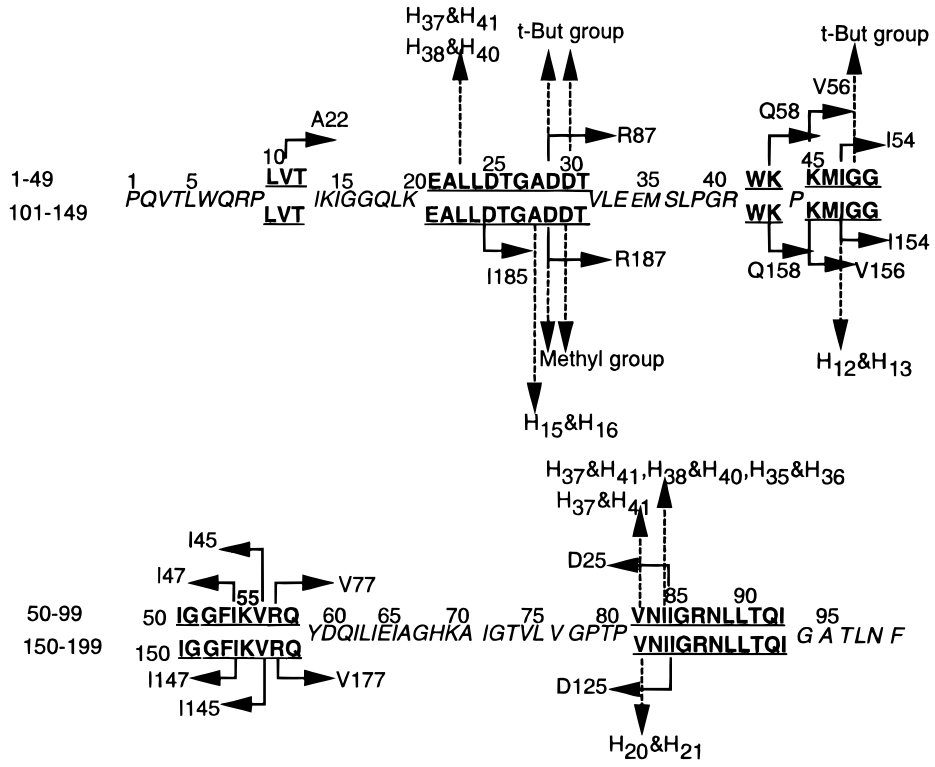


FIGURE 4: Schematic summary of NOEs used for the monomer-specific assignments. Upper case italic letters represent residues that are not monomer-specifically assigned. This could be due to chemical shift degeneracy or due to a lack of monomer-specific assignments even though the amide proton and nitrogen chemical shifts are not degenerate. Proline residues are also not monomer-specifically assigned. Underlined upper case boldface letters represent residues that are monomer-specifically assigned. Solid arrows indicate long-range NOEs, observed in the 3D $^{15}$N-edited NOESY spectrum. Dashed arrows indicate NOEs between protein protons and KNI-272 protons, observed in the 3D $^{13}$C-filtered $^{15}$N-edited NOESY and the $^{13}$C-filtered $^{13}$C-edited HMQC-NOESY spectra. The top strand represents monomer 1, residues 1−99; the bottom strand is monomer 2, residues 101−199.

to thiomethyl and *tert*-butyl protons, observed in the $^{13}$C-filtered/$^{15}$N-edited spectrum (Figure 3).

## RESULTS AND DISCUSSION

Assignments of $^{1}$H signals of KNI-272 and $^{1}$H, $^{13}$C, and $^{15}$N signals of the protease are listed in Tables S2 and S3, respectively, in the supporting information. The Asp C$^{\gamma}$ chemical shifts are plotted as a function of pD in Figure 5, and the values of p$K_a$, $\delta_{A^-}$, and $\delta_{AH}$ derived from the fits of this data are listed in Table 1.

As seen in Table 1, Asp30/130 have p$K_a$ values close 3.9, the value observed in a solvated model peptide. This result is in accord with the X-ray structure which shows that the Asp30/130 carboxyls are exposed to solvent. The p$K_a$ values of the solvent-exposed Asp60/160 carboxyl groups are a little less then those of Asp30 and Asp130 (Table 1).

Like the C$^{\gamma}$ signals of Asp30/60/130/160, the C$^{\gamma}$ signals of Asp29/129 shift downfield as the pD decreases from 5.2 to 2.5. At first sight this result appears to be a simple consequence of the shift in equilibrium toward the protonated form of the carboxyls. However, several observations suggest that the Asp29/129 titration data require further analysis. First, the Asp29/129 chemical shifts change by an unusually small amount, less than 1 ppm, rather than 3−4 ppm as normally observed for titrating Asp carboxyl carbons. It is possible that some, if not all, of the observed changes in the Asp29/129 C$^{\gamma}$ chemical shifts reflect their sensitivity to the changing protonation states of the adjacent Asp30/130 residues, since the carboxyl oxygens of Asp29/129 are only ~5 Å from those of Asp30/130, respectively, rather

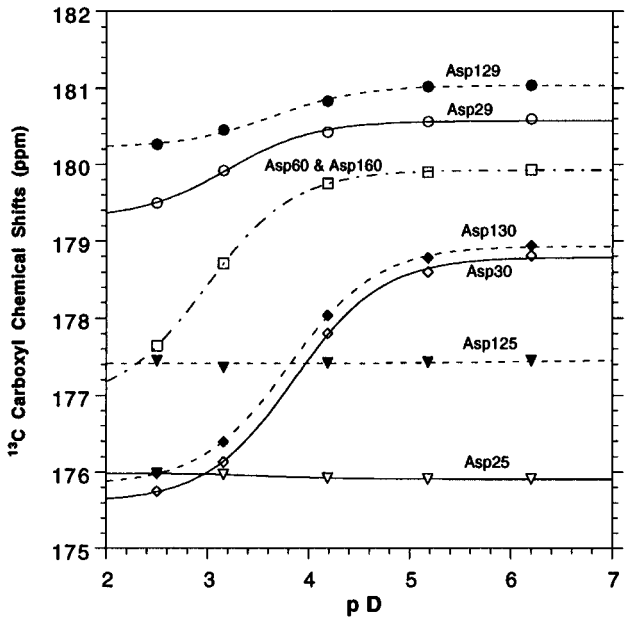


FIGURE 5: Chemical shifts of $^{13}$C carboxylate carbons of the protease/KNI-272 aspartic acids plotted as a function of pD. The pD is the meter reading, uncorrected for isotopic effects, and the fitted curves were obtained as described previously (Yamazaki et al., 1994b). The chemical shifts are indirectly referenced against the chemical shift of water at 45 °C (4.58 ppm). Note that Asp60 and Asp160 chemical shifts are degenerate.

than changes in their own protonation states. Indeed, at pD = 2.5 the chemical shifts of both Asp29/129 indicate that they are not protonated (Oda et al., 1993). Furthermore Asp29 and Asp129 form salt bridges with Arg108/87 and

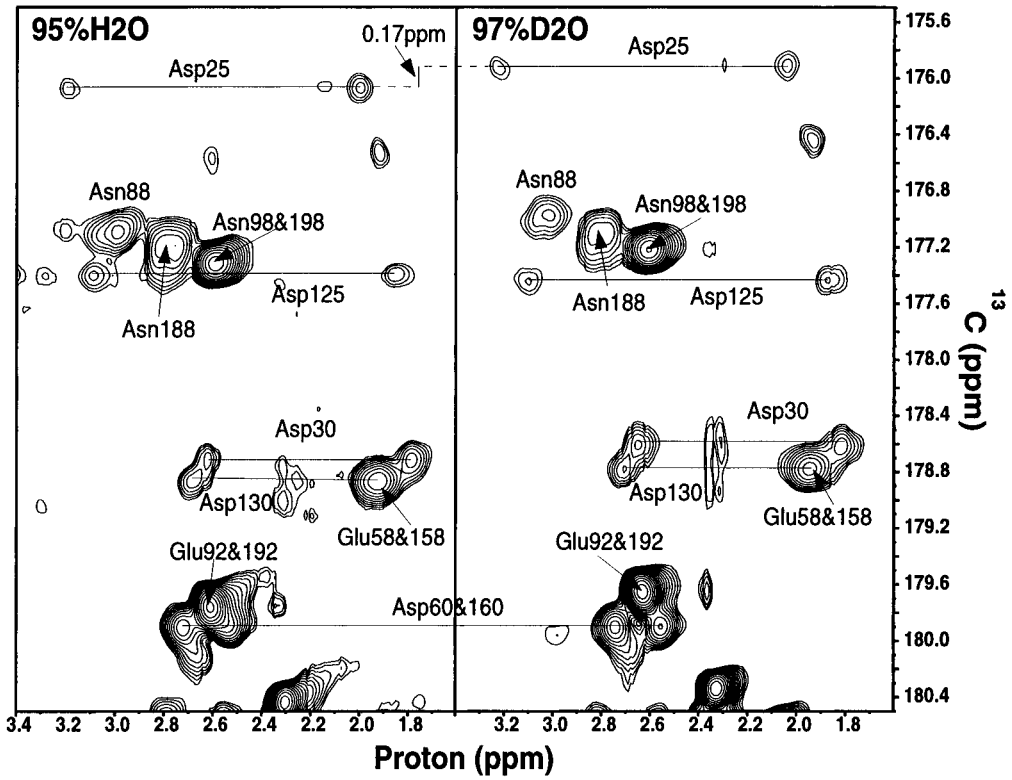


FIGURE 6: Comparison of HCABGCO spectra recorded in 95% $H_2O$/5% $D_2O$ and 97% $D_2O$/3% $H_2O$, demonstrating the isotope shift of Asp25. Note that the chemical shifts of Asp60 and Asp160 are the same in the two solvents because the Asp60 and Asp160 side chains are fully deprotonated at pD 5.2

Arg8/187, respectively (Baldwin et al., 1995), which are expected to significantly depress their p$K_a$ values (Oda et al., 1993). Unfortunately, we were only able to titrate the sample to pD = 2.5. At pD < 2.5 the complex begins to precipitate, and several attempts to obtain spectra at pD = 2.2 were not successful. Taken together, these results, suggest that the p$K_a$ values of Asp29 and Asp129 are probably below 2.5, and that protonation of these Asp residues may coincide with unfolding of the protein.

In contrast with the carboxyls of all other Asp residues, the C$^\gamma$ chemical shifts of Asp25 and Asp125 are essentially independent of pD in the range 2.5−6.2. This implies that p$K_a$ values of both aspartic acids lie outside the range of 2−7. These results are consistent with the crystal structure which shows that both Asp side chains are buried by the inhibitor and not accessible to bulk solvent. While the data in Figure 5 show clearly that the ionization states of Asp25 and Asp125 are independent of pD in the range from 2.5 to 6.2, the protonation states of the two Asp carboxyls remain to be determined. At pD 5.2, the Asp25 C$^\gamma$ is the most upfield shifted of all the Asp C$^\gamma$ signals, 175.9 ppm, immediately suggesting that the Asp25 carboxyl is protonated. This conclusion is strongly enforced by the observation that the Asp 25 C$^\gamma$ signal shifts (downfield) by +0.17 ± 0.02 ppm when the solvent is changed from 97% $D_2O$ to 95% $H_2O$ (Figure 6), corresponding to a 0.19 ± 0.02 ppm isotope shift (from neat $H_2O$ to neat $D_2O$), in good agreement with the 0.225 ± 0.015 ppm shift observed in model compounds (Ladner et al., 1975; Led & Petersen, 1979). In contrast, the signal of the carboxylate carbon of Asp125 experiences a small (upfield) shift of −0.05 ± 0.02 ppm upon changing solvent. The cause for this upfield shift (reverse isotope shift) is not known. However, we note that, in the crystal structure, both Asp 125 carboxyl oxygens accept hydrogen bonds, one from a bound water molecule and the other from the hydroxyl group of the KNI-272. The replacement of deuterium with hydrogen in these H-bonds could be the source of a small reverse isotope shift observed for the Asp125 carboxyl carbon. We further note that a negligible isotope shift, +0.01 ± 0.02 ppm, was observed for the signals of Asp60 and Asp160 which are deprotonated at pH 5.2, according to their low p$K_a$ values (Table 1), providing an internal control for the experiments.

Taken together our data show that Asp25 is protonated while Asp125 is deprotonated over the pD range extending

Table 1: Parameters Derived from Fitting[a] the Asp C$^\gamma$ Chemical Shift Titration Data[b]

| | Asp25 | Asp125 | Asp29 | Asp129 | Asp30 | Asp130 | Asp60 and Asp160 |
|---|---|---|---|---|---|---|---|
| p$K_a$ | >6.2[c] | <2.5[c] | 3.19[d] | 3.65[d] | 3.88 | 3.78 | 2.99 |
| $\delta_{A^-}$ | NA[e] | NA | 180.57 | 181.04 | 178.79 | 178.93 | 179.93 |
| $\delta_{AH}$ | NA | NA | 179.29 | 180.22 | 175.61 | 175.83 | 176.89 |

[a] Experimental data were fit with the function $\delta = \delta_{A^-} - (\delta_{A^-} - \delta_{AH})/(1 + 10^{(pD-pK_a)})$, where p$K_a$, $\delta_{A^-}$, and $\delta_{AH}$ are parameters derived from the fit. The latter two quantities are the respective chemical shifts in either the absence or the presence of a proton on the carboxyl oxygen. [b] The titration was limited to the pD range from 2.5 to 6.2 because the protein precipitates outside of this range. [c] Although the Asp25 C$^\gamma$ does not titrate in the pD range from 2.5 to 6.2, the isotope shift experiment shows that it is protonated throughout this range. The same experiment shows that the carboxyl group of Asp125 is deprotonated throughout the pD range. [d] Apparent p$K_a$ values, see the discussion in the text. Because the Asp29/129 chemical shifts are pH sensitive at pH = 2.5, and are expected to be sensitive to the protein aggregation/unfolding that begins at ca. this pH, the isotopic shift experiments were not performed at pH = 2.5. [e] Not applicable because the chemical shifts of Asp25/125 carboxyl groups do not titrate in the pD range from 2.5 to 6.2.

from 2.5 to 6.2. Our titration experiment could not be extended beyond this range because the protease/KNI-272 complex irreversibly precipitates at pD values outside this range. Our experimental results agree with the prediction of a semi-empirical quantum mechanical calculation on the ionic states of catalytic Asp residues of the HIV-1 protease/KNI-272 complex (Baldwin et al., 1995). According to their analysis, both oxygens of the side chain carboxyl group of Asp125 are deprotonated in order to accept two hydrogen bonds, one from a tightly bound water molecule (water 607) and another from a hydroxyl group on KNI-272. In contrast to Asp125, the side chain of Asp25 is protonated in order to donate a hydrogen bond to a carbonyl oxygen of KNI-272. These distinct protonation states of Asp25/125 also agree with protonation states proposed for the protease complexed with hydroxylethylene-containing inhibitors, in which one of Asp residues in the active site must be deprotonated in order to accept a hydrogen bond from the hydroxyl group of the inhibitors (Wlodawer & Erickson, 1993). On the other hand, the different protonation states observed herein for the Asp25/125 contrast with experimental results obtained for the protease/DMP323 complex (Yamazaki et al., 1994b), which showed that both Asp25/125 carboxyl groups are protonated in the pD range extending from 2.2 to 7.0. Hence, these studies enforce the idea that the protonation states of the catalytic Asp side chains depend strongly upon specific interactions with the inhibitor and imply that knowledge of these quantities is required for a detailed understanding of protease/drug interactions.

## ACKNOWLEDGMENT

We thank Frank Delaglio and Dan Garrett for providing NMR data analysis software, Rolf Tschudin for expert technical support, and Ann Frances Miller and Michelle Markus for their critical reviews of the manuscript. We also thank John W. Erickson for kindly providing the coordinates of the X-ray crystal structure of the HIV-1 protease/KNI-272 complex prior to their publication.

## SUPPORTING INFORMATION AVAILABLE

List of experiments applied to assign the $^{1}H$, $^{13}C$, and $^{15}N$ signals of the HIV-1 protease/KNI-272 complex (Table S1); proton chemical shifts of inhibitor KNI-272 (Table S2); chemical shift assignments of the $^{1}H$, $^{13}C$, and $^{15}N$ signals of the HIV-1 protease/KNI-272 complex (Table 3S); and KNI-272 chemical structure and numbering scheme (Figure S1) (10 pages). Ordering information is given on any current masthead page.

## REFERENCES

Baldwin, E. T., Bhat, T. N., Gulnik, S., Liu, B., Topol, I. A., Kiso, Y., Mimoto, T., Mitsuya, H., & Erickson, J. W. (1995) *Structure 3*, 581−590.

Bundi, A., & Wüthrich, K. (1979) *Biopolymers 18*, 285−297.

Burgering, M. J. M., Boelens, R., Caffrey, M., Breg, J. N., & Kaptein, R. (1993) *FEBS Lett. 330*, 105−109.

Chokeijichai, S., Shirasaka, T., Weinstein, J. N., & Mitsuya, H. (1995) *Antiviral Res. 28*, 25−38.

Delaglio, F., Grzesiek, S., Vuister, G. W., Zhu, G., Pfeifer, J., & Bax, A. (1995) *J. Biomol. NMR 6*, 277−293.

Harte, W. E., Jr., & Beveridge, D. L. (1993) *J. Am. Chem. Soc. 115*, 3883−3886.

Huff, J. R. (1991) *J. Med. Chem. 34*, 2305−2314.

Ikura, M., & Bax, A. (1992) *J. Am. Chem. Soc. 114*, 2433−2440.

Kageyama, S., Mimoto, T., Murakawa, Y., Nomizu, M., Ford, H. J., Jr., Shirasaka, T., Gulnik, S., Erickson, J., Takada, K., Hayashi, H., Broder, S., Kiso, Y., & Mitsuya, H. (1993) *Antimicrob. Agents Chemother. 37*, 810−817.

Kiso, Y. (1996) *Biopolymers* (in press).

Ladner, H. K., Led, J. J., & Grant, D. M. (1975) *J. Magn. Reson. 20*, 530−534.

Lam, P. Y., Jadhav, P. K., Eyermann, C. J., Hodge, C. N., Ru, Y., Bacheler, L. T., Meek, J. L., Otto, M. J., Rayner, M. M., Waong, Y. N., Chang, C.-H., Weber, P. C., Jackson, D. A., Sharpe, T. R., & Erickson-Viitanen, S. (1994) *Science (Washington, D. C.) 263*, 380−384.

Led, J. J., & Petersen, S. B. (1979) *J. Magn. Reson. 33*, 603−617.

Oda, Y., Yamazaki, T., Nagayama, K., Kanaya, S., Kuroda, Y., & Nakaumra, H. (1993) *Biochemistry 33*, 5275−5284.

Wlodawer, A., & Erickson, J. W. (1993) *Annu. Rev. Biochem. 62*, 543−585.

Wlodawer, A., Miller, M., Jaskolski, M., Sathyanrayana, B. K., Baldwin, E., Weber, I. T., Selk, L. M., Clawson, L., Schneider, J., & Kent, S. B. H. (1989) *Science (Washington, D. C.) 245*, 616−621.

Yamazaki, T., Nicholson, L., Torchia, D. A., Stahl, S. J., Kaufman, J. D., Wingfield, P. T., Domaille, P. J., & Campbell-Burk, S. (1994a) *Eur. J. Biochem. 219*, 707−712.

Yamazaki, T., Nicholson, L. K., Wingfield, P. T., Stahl, S. J., Haufman, J. D., Lam, P. Y. S., Ru, Y., Jadhav, P. K., Chang, C.-H., Weber, P. C., & Torchia, D. A. (1994b) *J. Am. Chem. Soc. 116*, 10791−10792.

Yamazaki, T., Hinck, A. P., Wang, Y.-X., Nicholson, L. K., Torchia, D. A., Wingfield, P. T., Stahl, S. J., Kaufman, H. D., Chang, C.-H., Domaille, P. J., & Lam, P. Y. S. (1996) *Protein Sci. 5*, 495−506.

BI961268Z